Peroxisome proliferator-activated receptor-γ coactivator 1-α (PGC1α) is a metabolic regulator of intestinal epithelial cell fate

Ilenia D'Errico[a,b], Lorena Salvatore[a,b], Stefania Murzilli[a,b], Giuseppe Lo Sasso[a,b], Dominga Latorre[c], Nicola Martelli[a,b], Anastasia V. Egorova[d], Roman Polishuck[d], Katja Madeyski-Bengtson[e], Christopher Lelliott[f], Antonio J. Vidal-Puig[g], Peter Seibel[h], Gaetano Villani[c], and Antonio Moschetta[a,b,1]

[a]Laboratory of Lipid Metabolism and Cancer, Department of Translational Pharmacology, Consorzio Mario Negri Sud, 66030 Santa Maria Imbaro, Chieti, Italy; [b]Clinica Medica "A. Murri," University of Bari, 70124 Bari, Italy; [c]Department of Medical Biochemistry, Biology, and Physics, University of Bari, 70124 Bari, Italy; [d]Department of Cell Biology and Oncology, Consorzio Mario Negri Sud, 66030 Santa Maria Imbaro, Chieti, Italy; [e]AstraZeneca Transgenic and Comparative Genomics, AstraZeneca Research and Development, SE-43183 Mölndal, Sweden; [f]Department of Biosciences, AstraZeneca Research and Development, SE-43183 Mölndal, Sweden; [g]Metabolic Research Laboratories, Institute of Metabolic Science, University of Cambridge, Cambridge CB2 0QQ, United Kingdom; and [h]Department of Molecular Cell Therapy, Center for Biotechnology and Biomedicine, University of Leipzig, 04103 Leipzig, Germany

Edited* by David J. Mangelsdorf, University of Texas Southwestern Medical Center, Dallas, TX, and approved March 10, 2011 (received for review November 9, 2010)

Peroxisome proliferator-activated receptor-γ coactivator 1-α (PGC1α) is a transcriptional coactivator able to up-regulate mitochondrial biogenesis, respiratory capacity, oxidative phosphorylation, and fatty acid β-oxidation with the final aim of providing a more efficient pathway for aerobic energy production. In the continuously renewed intestinal epithelium, proliferative cells in the crypts migrate along the villus axis and differentiate into mature enterocytes, increasing their respiratory capacity and finally undergoing apoptosis. Here we show that in the intestinal epithelial surface, PGC1α drives mitochondrial biogenesis and respiration in the presence of reduced antioxidant enzyme activities, thus determining the accumulation of reactive oxygen species and fostering the fate of enterocytes toward apoptosis. Combining gain- and loss-of-function genetic approaches in human cells and mouse models of intestinal cancer, we present an intriguing scenario whereby PGC1α regulates enterocyte cell fate and protects against tumorigenesis.

colon cancer | medical physiology | metabolism | mitochondria | nuclear receptors

The intestinal epithelium is a dynamic microenvironment in which proliferative progenitor cells in the crypt give rise to epithelial cells that differentiate into mature enterocytes while migrating to the intestinal lumen (1). Current evidences indicate the well-known Wnt/β-catenin pathway (2) as the main force in the regulation of the crypt-villus homeostasis. Under physiological conditions, intestinal epithelial cells, migrating from the crypt to the top of the villus, reduce their proliferative activity and modify their metabolic behavior, becoming competent for apoptosis (1, 3). When a somatic mutation occurs, some cells are able to escape apoptosis, thus promoting tumor progression (4, 5).

Peroxisome proliferator-activated receptor-γ coactivator 1-α (PGC1α) is a transcriptional coactivator of genes encoding proteins responsible for the regulation of mitochondrial biogenesis and function (6, 7). PGC1α participates in biological responses that require the shift from glycolytic to oxidative metabolism, such as thermogenesis in brown adipose tissue (8), fiber-type switching in skeletal muscle (9), and fatty acid β-oxidation, along with gluconeogenesis, in the liver (10). Despite the large amount of information about the role of PGC1α in high energy-demand tissues, nothing has yet been reported about the role of PGC1α in the intestine. Therefore, we sought to explore whether PGC1α may influence the metabolic fate of intestinal epithelial cells.

Here we show that PGC1α is highly expressed on the surface of the intestinal epithelium, where cells accumulate reactive oxygen species (ROS), probably due to the unbalanced ratio between increased respiration and lower activity of the antioxidant enzymes. In contrast, PGC1α is poorly expressed in the crypts, and its expression is reduced in intestinal tumors. In highly glycolytic proliferative colorectal cancer cells, PGC1α overexpression induces a turbo boost of the mitochondrial machinery with ROS accumulation and apoptosis. Intriguingly, mice overexpressing PGC1α in the intestinal epithelium are strongly protected against tumorigenesis, whereas the opposite is observed in PGC1α$^{-/-}$ mice. Thus, we propose that PGC1α, reinforcing the physiological effect produced by the expansion of mitochondrial population and function in the intestinal epithelium, could be considered a metabolic regulator of intestinal cell fate and a putative powerful tool against intestinal tumor formation.

Results

PGC1α Is Highly Expressed in the Intestinal Epithelium. We first investigated the expression level of *PGC1α* in the intestine analyzing mRNA transcripts from mice tissues. We found significant *PGC1α* levels in the entire gastrointestinal tract (Fig. 1*A*). Notably, PGC1α is localized in the differentiated enterocytes that belong to the apical compartment of the epithelium. Conversely, PGC1α has only a scattered expression in the proliferative compartment at the bottom of the crypts (Fig. 1*B*, red arrows). Intriguingly, PGC1α expressing apical differentiated enterocytes present a higher respiratory capacity, as evaluated via COX activity (Fig. 1*C*). In situ measurement of COX activity by histochemical staining is an indication for respiratory capacity (11–13). Furthermore, ROS accumulation (Fig. 1*D*) has been detected in the same compartment that results in a susceptibility to apoptosis (Fig. 1*E*), probably due to low expression of antioxidant enzymes catalase (CAT) and manganese superoxide dismutase (SOD2; Fig. S1) (14, 15).

We then measured its abundance in intestinal tumor samples from mice and familial adenomatous polyposis (FAP) patients. In both cases, intestinal adenomas result from mutational activation of the Wnt pathway (16), most commonly due to the loss of the intestinal tumor suppressor gene *Apc* (4, 17–19). In colon tumor samples from Apc$^{Min/+}$ mice and FAP patients, mRNA levels of *PGC1α* and its target, medium-chain acyl-CoA dehydrogenase (*MCAD*) were 70–90% lower than the mRNA levels of the adjacent intestinal mucosa, similar to the expression pattern of differentiation marker genes such as *p21* and *Keratin20* (Fig. 1*F*).

Author contributions: I.D. and A.M. designed research; I.D., L.S., S.M., G.L.S., N.M., R.P., K.M.-B., C.L., A.J.V.-P., P.S., and G.V. performed research; L.S., S.M., G.L.S., D.L., N.M., A.V.E., R.P., K.M.-B., C.L., A.J.V.-P., P.S., and G.V. contributed new reagents/analytic tools; D.L., A.V.E., C.L., A.J.V.-P., P.S., G.V., and A.M. analyzed data; and I.D., G.V., and A.M. wrote the paper.

The authors declare no conflict of interest.

*This Direct Submission article had a prearranged editor.

[1]To whom correspondence should be addressed. E-mail: moschetta@negrisud.it.

This article contains supporting information online at www.pnas.org/lookup/suppl/doi:10.1073/pnas.1016354108/-/DCSupplemental.

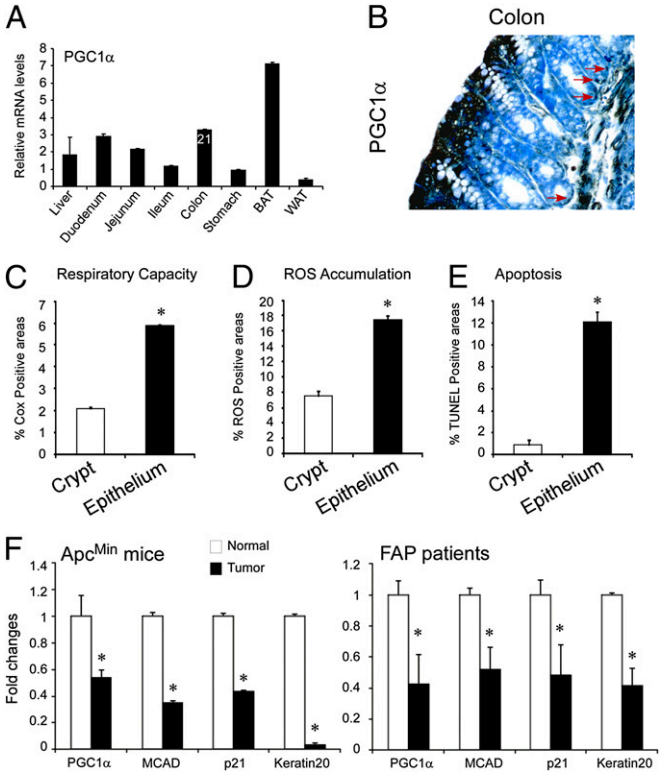

Fig. 1. PGC1α expression levels and localization in normal intestinal epithelium and tumors. (*A*) PGC1α mRNA expression was measured by real-time-qPCR. Results are expressed as mean ± SEM. Mean cycle threshold (Ct) of colon samples is reported in number. BAT, brown adipose tissue; WAT, white adipose tissue. (*B*) PGC1α is strongly expressed in the apical-differentiated enterocytes of the colon epithelium, and red arrows depict the few PGC1α-expressing cells at the basis of the crypt (200× magnification). (*C*) Intestinal activity of COX was measured on frozen colon samples from WT mice. Images were quantified using ImageJ software. (*D*) ROS accumulation was measured on frozen colon samples from WT mice. Images were quantified using the ImageJ software. (*E*) Apoptosis on colon from WT mice was evaluated by TUNEL assay on paraffin-embedded samples. (*F*) Decreased mRNA levels of *PGC1α*, *MCAD*, *p21*, and *Keratin20* were detected in tumors of $Apc^{Min/+}$ mice and FAP patients compared with the normal adjacent mucosa. Results are expressed as mean ± SEM. Cyclophilin was used as a reference gene, and values were normalized to data obtained from normal intestinal mucosa (*$P < 0.05$).

PGC1α Induces Mitochondrial Proliferation and Activation in Human Intestinal Cancer Cells. Switching mitochondrial activity is a putative form of cancer therapy (20, 21). We explored whether PGC1α expression induces metabolic remodeling and/or modifies cell behavior in an undifferentiated and proliferative intestinal tumor cell. Overexpression of PGC1α in HT29 cells markedly activated its transcriptional machinery, as shown by the increase in the expression of several target genes—namely, *MCAD*, mitochondrial transcription factor A (*Tfam*), and ATP synthase β-subunit (*ATP5B*; Fig. 2*A*). This gene expression scenario was accompanied by metabolic changes. Indeed, though no changes were observed in the glycolysis rate using [5-^{3}H]glucose as a substrate (Fig. 2*B*), there was a significant increase in mitochondrial fatty acid β-oxidation, as shown by the [9,10-^{3}H] palmitic acid oxidation rate (Fig. 2*C*). We also observed a net expansion of the mitochondrial population, indicated by increased mtDNA molecules and MitoTracker staining (Fig. 2 *D* and *E*), followed by an increase in oxygen consumption (Fig. 2*F*) calculated on cells without cytochrome *c* (cyt *c*) efflux (22). PGC1α overexpression produced a proapoptotic effect, highlighted by Annexin V staining (Fig. 2*G* and Fig. S2*A*) and cyt *c* efflux (Fig. S2*B*). Under these conditions, cells decrease their proliferative rate (Fig. S2*C*). These data suggest that PGC1α promotes a coordinate metabolic shift toward mitochondrial utilization in proliferative cancer cells.

PGC1α Induces Tissue-Specific ROS Accumulation and Apoptosis. The correct balance between ROS production and the antioxidant systems maintains cellular ROS homeostasis. We thus first measured ROS accumulation after PGC1α overexpression in colorectal cancer cells (HT29 and HCT116) and in nonintestinal cells (143B and C2C12; Fig. 2*H*). We observed a very high percentage of ROS-positive cells only in intestinal cancer cells; neither 143B nor C2C12 cells accumulated ROS. The levels of ROS accumulation were completely paralleled by the nucleosome-enrichment observed in the same cells as a sign of apoptosis (23) (Fig. 2*I*). In response to PGC1α overexpression, only 143B and C2C12 showed a significant increase in antioxidant enzymes CAT and SOD2 (Fig. S1*A*). In tissues with high aerobic energy metabolism, such as brain, heart, skeletal muscle, and brown adipose tissues (6–9, 24, 25), where PGC1α expression responds to specific stimuli determining the increase in mitochondrial activity, a parallel increase in antioxidant enzyme production (i.e., SOD2 and CAT) occurs to protect cells from oxidative stress. In contrast, colorectal cancer cells did increase their antioxidant defense, thus becoming apoptotic. Our data suggest that the metabolic shift induced by PGC1α in proliferative colorectal cancer cells promotes ROS accumulation and induces apoptosis.

PGC1α Inhibits Intestinal Tumor Growth in a Xenograft Model. Interfering with the glycolytic metabolic scenario of tumor cells can prevent tumor onset and reduce tumor growth (21, 26). To prove if the proapoptotic PGC1α mitochondrial-driven activity is able to oppose tumorigenesis, we performed a xenograft model in athymic mice using HT29 cells. Adenoviral infection of tumors with PGC1α produced a strong reduction of tumor growth. Indeed, tumors overexpressing PGC1α display a significant delay in their growth compared with mock-treated tumors (Fig. 2*J*). Tumors infected with PGC1α presented a net increase in COX staining, indicating activation of mitochondrial respiration (Fig. 2*K*). The PGC1α mediated induction of mitochondrial respiration resulted in a net accumulation of ROS with a consequent increase of apoptosis (Fig. 2*K*).

PGC1α Proapoptotic Effect Is Lost in HT29ρ0 Cells. To investigate whether the observed ROS boost after PGC1α overexpression was really due to the increased activity of the respiratory chain, we introduced in our study a cellular model that completely lacks mitochondrial DNA (HT29ρ0 cells). This mtDNA-depleted cell line was generated by ethidium bromide treatment (27). To verify the complete removal of the mtDNA, the total genomic DNA of the HT29ρ0 cells was used as a template in a multiplex PCR test to amplify both the nuclear actin gene and the mtDNA-encoded cytochrome *b* (*cyt b*) gene (Fig. 3*A*). As shown, the mitochondrial *Cytb* gene was amplified only in HT29 WT cells. Through Western blot analysis (Fig. 3*A*) we have also confirmed that the mitochondrial-encoded cyt *c* oxidase subunit I (COXI) was expressed only in HT29 WT but not in HT29ρ0 cells. To further confirm the bioenergetic functional impact of the mtDNA absence in HT29ρ0 cells, we measured mitochondrial respiratory fluxes in HT29 WT and HT29ρ0 cells (Fig. 3*B*). As expected, no antimycin-sensitive oxygen consumption could be detected in intact HT29ρ0 cells in the presence (basal) or in the absence (DNP uncoupled) of the mitochondrial membrane potential. Similarly, no COX activity could be detected in intact HT29ρ0 cells as KCN-sensitive oxygen consumption elicited by the artificial COX-specific electron donors ascorbate + TMPD (Fig. 3*B*) or as in vitro enzyme activity measured in cell lysate (0 vs. 24.5 ± 1.1 nmol·mg^{-1}·min^{-1}, HT29ρ0 vs. HT29 cells). On the contrary, the citrate synthase activity, a nuclear-encoded mitochondrial citric acid cycle enzyme, is still present in HT29ρ0 cells (94 ± 16.9 vs. 74 ± 33.3 nmol·mg^{-1}·min^{-1}, HT29ρ0 vs. HT29 cells).

We then overexpressed PGC1α in both HT29 and HT29ρ0 cells and compared the transcriptional activation of several PGC1α target genes, such as *MCAD*, *Tfam*, and *ATP5B*. As shown in Figs. 2*A* and 3*C*, all of these genes are activated in both cell lines, thus

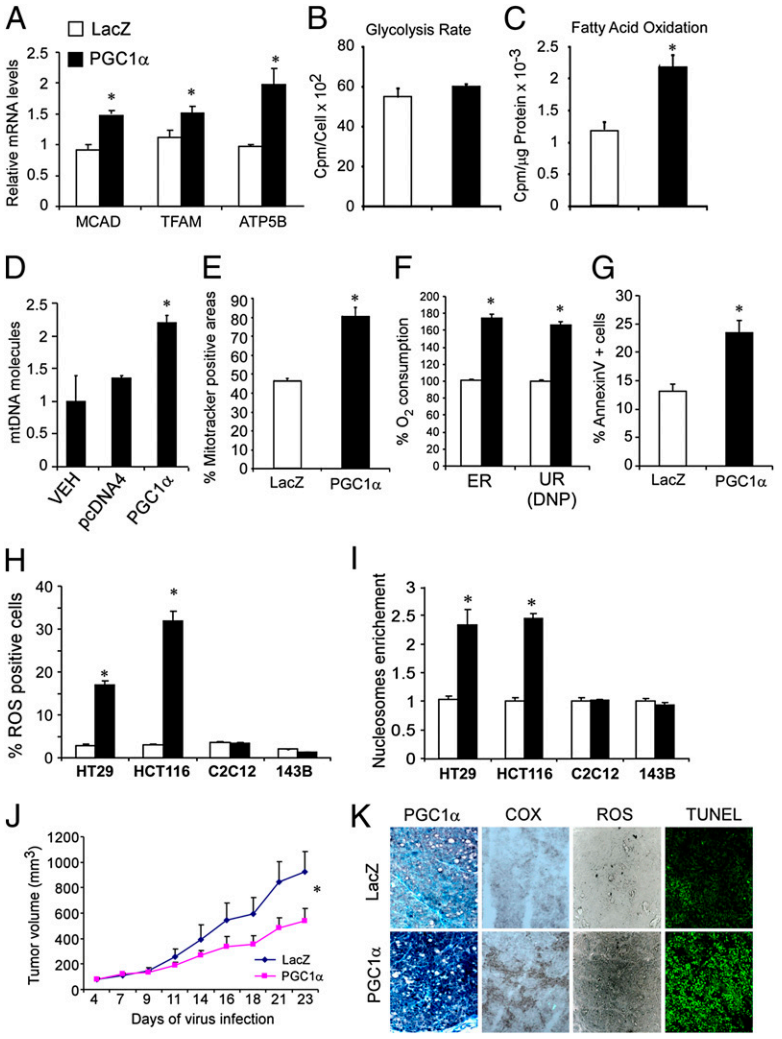

Fig. 2. PGC1α induces apoptosis in colorectal cancer cells. (*A*) HT29 cells were infected with PGC1α adenovirus (AdPGC1α) and AdLacZ as control for 48 h. Cells were analyzed for relative expression levels of PGC1α target genes *MCAD*, *Tfam*, and *ATP5β* by real-time qPCR. Values shown represent mean ± SEM. (*B*) A PGC1α increase does not alter the glycolysis rate in HT29 cells. Cells were infected with AdPGC1α (AdlacZ as control) and cultured in medium containing [5-^{3}H]glucose. Glycolysis rate was assessed by measuring ^3H_2O produced in the incubation medium by liquid scintillation counting. (*C*) PGC1α overexpression induces fatty acid oxidation in HT29 cells. Cells were infected with AdPGC1α (AdlacZ as control) and cultured in medium containing [9,10-^{3}H]palmitic acid. Palmitic oxidation was assessed by measuring ^3H_2O produced in the incubation medium by liquid scintillation counting. (*D*) Determination of the relative mtDNA level in HT29 cells transfected with pCDNA-PGC1α or empty pCDNA4 as control for 48 h. Cells were analyzed for relative COX2 mitochondrial levels by real-time qPCR, and actin was used as a nuclear reference gene. (*E*) At 48 h after PGC1α adenoviral infection, HT29 cells were stained with MitoTracker Red 580 to evaluate the increase in the mitochondrial population. (*F*) PGC1α overexpression determines the increase in both endogenous (ER) and uncoupled (UR) mitochondrial respiration in HT29 cells. Mitochondrial respiration was expressed as a percentage of oxygen consumption. (*G*) HT29 cells were infected AdPGC1α or AdLacZ as control. After 48 h, cells were incubated with Annexin V-Alexa (red) and propidium iodide. The fluorescence of cells was immediately determined with a flow cytometer. (*H*) PGC1α overexpression determines ROS accumulation in intestinal cells. Colorectal cancer cells HT29 and HCT116, mouse myoblast cells C2C12, and osteosarcoma cells 143B have been infected with AdPGC1α and AdLacZ for 48 h. Intracellular ROS levels were determined using CM-H_2DCFDA (Molecular Probes, Invitrogen), and the levels of fluorescence were immediately detected using flow cytometry. (*I*) PGC1α overexpression induces apoptosis in intestinal cells. The cytoplasmatic levels of nucleosomes derived from AdPGC1α-and AdLacZ-infected HT29, HCT116, C2C12, and 143B cells were evaluated after 48 h by photometric analysis (405 nm). Each measurement was normalized to the protein content of the cells. (*J*) Athymic Nu/Nu mice were s.c. injected with HT29 cells, and AdPGC1α or AdLacZ was directly subministrated inside the tumor mass. A tumor growth delay was observed in tumors treated with AdPGC1α compared with AdLacZ. (*K*) Cox and ROS activities on frozen tumor sections from AdPGC1α- and AdLacZ-infected tumors were assayed by histochemistry assays. A TUNEL assay was performed on paraffin-embedded samples. PGC1α-treated tumors show high COX activity, ROS accumulation, and apoptosis.

proving that PGC1α transcriptional activity is fully conserved in HT29ρ0 cells. PGC1α promoted significant ROS accumulation in HT29 WT cells but not in HT29ρ0 cells (Fig. 3*C*). Moreover, in addition to ROS accumulation, marked nucleosome enrichment also occurred in HT29 WT but not HT29ρ0 cells (Fig. 3*C*). These findings support our hypothesis that the proapoptotic effect exerted by PGC1α is tightly related to the increased mitochondrial respiratory chain activity and subsequent intestinal-specific ROS accumulation.

Synthetic SOD2 and Catalase Mimetic EUK134 Abolishes the PGC1α Proapoptotic Effect. We then studied the effect of PGC1α overexpression in colorectal cancer cells and xenografted tumors in the presence of a synthetic combined catalase and SOD2 mimetic referred to as EUK134 (28). Treatment of colorectal cancer cells, and of xenografted tumors with EUK134, completely prevented the PGC1α-induced proapoptotic and tumor-suppressor activity. At a molecular level, PGC1α overexpression in the presence of EUK134 did not lead to ROS accumulation and apoptosis (Fig. 3*D*). Furthermore, EUK134 prevented a PGC1α-induced reduction in tumor growth rate as well as ROS accumulation and apoptosis in vivo (Fig. 3*E*). These data support the model by which the intestinal PGC1α proapoptotic effect depends on the imbalance between increased mitochondrial respiratory capacity and decreased free radical scavenger systems.

PGC1α Stimulates Intestinal Mitochondrial Biogenesis and Respiration in Vivo. To translate the relevance of these effects in the physiological context of the intestinal epithelium, we generated a mouse model in which human PGC1α (hPGC1α) is selectively overexpressed only in the intestinal cells. Thus, by subcloning the *hPGC1α* coding sequence downstream of the villin promoter, we generated the iPGC1α transgenic mice. These mice express the *hPGC1α* transgene in the entire length of their intestines (Fig. 4 *A* and *B*). The apical enterocytes of the iPGC1α intestine show an evident increase in the number of mitochondria, as revealed by EM pictures and the percentage of COX-1 staining-positive areas (Fig. 4 *C* and *D*). This constitutive PGC1α expression in the normal intestinal epithelium is thus able to activate mitochondrial biogenesis and activity leading in vivo to ROS accumulation (Fig. 4*D*). iPGC1α mice presented a higher number of TUNEL-positive cells surrounding the entire surface of the villi, showing a highly sensitive apoptotic profile if compared with WT mice (Fig. 4*D*). The proapoptotic phenotype produced by PGC1α intestinal expression is also reflected by some morphological differences in colon and ileum sections of iPGC1α, PGC1α$^{+/+}$, and PGC1α$^{-/-}$ mice. The three different genotypes showed striking differences in the dimension of villi and crypts, which were visibly shorter in iPGC1α mice compared with PGC1α$^{+/+}$ and, even more, with PGC1α$^{-/-}$ mice (Fig. S3 and Fig. S4). Therefore, higher accumulations of ROS on the surface

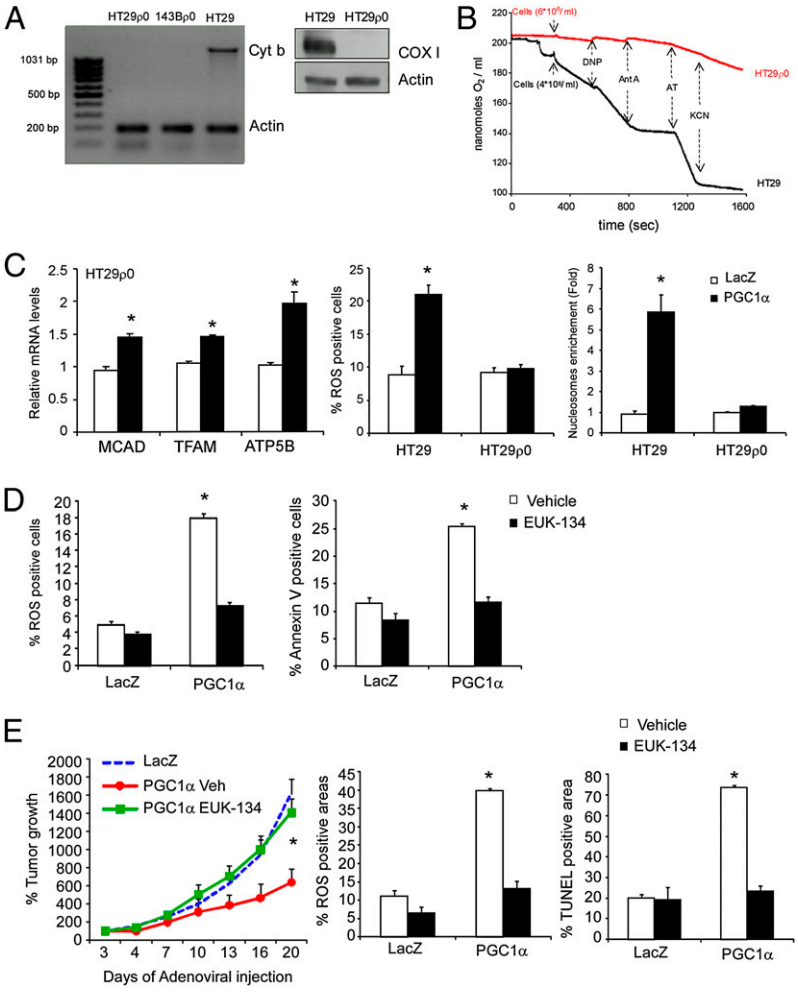

Fig. 3. PGC1α proapoptotic effect in colorectal cancer cells is abolished in HT29ρ0 cells. (*A*) Amplification of mtDNA (*cyt b*) and nuclear (*actin*) genes by multiplex PCR in HT29 WT, HT29ρ0, and 143BTKρ0 cell lines (control cells). Western blot analysis of the mtDNA-encoded (*mit*) subunit I of COXI and of the nuclear-encoded β-actin (*nuc*) in HT29 WT and HT29ρ0 total cell lysates. (*B*) Representative oxygraphic tracings of respiratory fluxes by endogenous substrates in intact HT29 and HT29ρ0 cells. *DNP*, 2,4-dinitrophenol (60 μM); *Ant A*, antimycin A (40 nM); *AT*, ascorbate (10 mM) plus *N,N,N′, N′*-tetramethyl-*p*-phenylenediamine (0.4 mM); *KCN*, potassium cyanide (2 mM). (*C*) HT29 and HT29ρ0 cells were infected with AdPGC1α and AdLacZ as a control for a prolonged period (72 h). Cells were then analyzed for relative expression levels of PGC1α target genes *MCAD*, *Tfam*, and *ATP5β* by real-time qPCR. PGC1α overexpression determines ROS accumulation in HT29 but not in HT29ρ0 cells infected with AdPGC1α compared with AdLacZ. The cytoplasmatic levels of nucleosomes (apoptosis) are increased in AdPGC1α-infected HT29 but not in HT29ρ0 cells compared with the AdLacZ-infected control cells. (*D*) HT29 cells were infected with AdPGC1α and AdLacZ as a control for 48 h. EUK134 and DMSO (vehicle) 2.5 μM were added to the culture medium. Cells were analyzed for ROS accumulation and Annexin V-FACS analysis. PGC1α overexpression in the presence of EUK134 does not lead to ROS accumulation and apoptosis. (*E*) Nude mice xenograft experiment. EUK134 and DMSO (vehicle) 2.5 μM in DMEM were administrated into tumors 2 h before adenoviral treatment during the entire procedure. EUK134 prevented PGC1α-induced reduction in tumor growth rate as well as apoptosis in vivo.

of iPGC1α intestinal epithelium, if not balanced by antioxidant enzyme activity, induce massive apoptotic events.

Intestinal PGC1α Suppresses Colorectal Carcinogenesis. We next tested the hypothesis that PGC1α might be a unique player in the prevention of intestinal tumorigenesis on two different models of intestinal carcinogenesis. A genetic model of intestinal tumor formation was generated by crossing $Apc^{Min/+}$ mice (19) with our iPGC1α mice. The second model consisted of a single i.p. injection with azoxymethane (AOM) to initiate cancer by alkylation of DNA facilitating base mispairings (29), followed by three cycles of oral dextran sodium sulfate (DSS) to sustain the intestinal tumor progression via induction of colitis (30). In the adenomas of iPGC1α/$Apc^{Min/+}$ mice that show significant expression of hPGC1α transgene (Fig. 5 *A* and *B*), we observed a higher apoptosis rate compared with tumors of control mice (Fig. 5*C*). Indeed, given the reduced SOD staining and mRNA levels in tumors (Fig. S1*B*), the PGC1α mediated increase of mitochondrial respiration leads to ROS accumulation. The data obtained in the genetic model proved that the average tumor number and volumes were considerably lower in each intestinal tract (duodenum, jejunum, ileum, and colon) from iPGC1α/$Apc^{Min/+}$ mice compared with their littermate controls (Fig. 5 *D* and *E*), thus confirming that PGC1α protects against intestinal tumorigenesis. Furthermore, in the chemical model, iPGC1α mice presented a significantly lower average tumor number than their littermate controls (Fig. 5*F*). Also, though WT mice developed colon tumors with an average volume of 15 mm^3, the few tumors in iPGC1α mice had an average volume of 4 mm^3.

$PGC1\alpha^{-/-}$ Mice Are Susceptible to Intestinal Tumorigenesis. We then analyzed the effect of PGC1α depletion on the occurrence of intestinal tumors by performing the AOM/DSS protocol on $PGC1\alpha^{+/+}$ and $PGC1\alpha^{-/-}$ mice. $PGC1\alpha^{-/-}$ mice presented a significantly higher tumor number than their littermate controls (Fig. 5*G*). Also, whereas $PGC1\alpha^{+/+}$ mice developed tumors of an average volume of ∼2 mm^3 in the colon, the tumors in $PGC1\alpha^{-/-}$ mice had an average volume of ∼10 mm^3.

Together, these data strongly support the idea that PGC1α expression levels could influence intestinal epithelial cell fate by inducing mitochondrial-related metabolic modifications that induce apoptosis. Nonetheless, unique antitumoral-specific PGC1α target gene pathways in the intestine could have also contributed to this scenario. Notably, a microarray expression profile analysis performed on intestines of iPGC1α, $PGC1\alpha^{+/+}$, and $PGC1\alpha^{-/-}$ mice revealed that no apoptotic-specific pathways appear to be transcriptionally modulated by PGC1α expression levels. Table S1 reports the mRNA expression levels of an array of genes involved in the apoptotic process, along with their fold modification. The gene expression-related pathways susceptible to PGC1α amounts in the mouse intestinal epithelium are therefore entirely involved in cell metabolic control and differentiation, most likely driven by PPAR-γ (31) and estrogen-related receptor-α (32) (Fig. S5 and Table S2).

Discussion

This work shows that the nuclear receptor coactivator PGC1α is abundantly expressed in the apical apoptosis-competent compartment of the intestinal epithelium, and that its up-regulation in normal intestinal mucosa and proliferating cancer cells exerts a unique proapoptotic and tumor suppressor role. Several nuclear receptors that interact with PGC1α, such as PPAR-γ (Table S2)

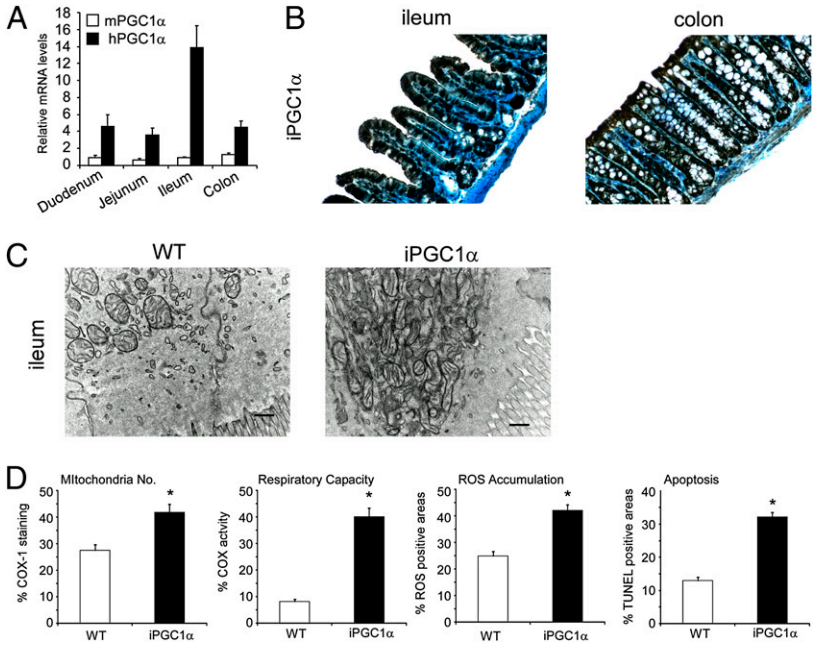

Fig. 4. Intestinal PGC1α overexpression promotes mitochondrial biogenesis and activities inducing apoptosis. (*A*) hPGC1α and mPGC1α relative mRNA expression from intestinal specimens of iPGC1α mice were measured by RT-qPCR. Results are expressed as mean ± SEM. (*B*) Paraffin-embedded terminal ileum and proximal colon specimens from iPGC1α mice were immunoassayed with PGC1α antibody to determine expression and localization of the protein (200× magnification). (*C*) Mitochondrial biogenesis was analyzed by performing transmission electron microscopy of thin sections prepared from WT and iPGC1α mice. (Scale bars: 320 nm.) (*D*) The expression of Oxphos COXI was analyzed by immunohistochemistry to highlight the mitochondrial content of normal sections of the ileum and colon from transgenic (iPGC1α) and WT mice. Intestinal activity of COX and ROS accumulation were measured on frozen ileum and colon samples from iPGC1α and WT mice. Images were quantified using ImageJ software. Apoptosis on ileum and colon from transgenic (iPGC1α) and WT mice was evaluated by TUNEL assay on paraffin-embedded samples.

(33–35), farnesoid X receptors (FXRs) (36), retinoic acid receptors (RARs), and retinoid X receptors (RXRs) (37), modulate both differentiation and apoptotic pathways in the intestine with a potential pharmacological importance in colon cancer (38).

Our study started from the consideration that in all of the tissues in which PGC1α is expressed, it increases mitochondrial biogenesis and activity (8–10). Thus, we explored whether PGC1α modulation could influence the metabolic fate of intestinal epithelial cells. PGC1α overexpression is not only able to stimulate mitochondrial biogenesis and metabolic activities in both colorectal cancer cells and murine intestines, it is also responsible for the accumulation of free radicals. ROS production is proportional to the increase in mitochondrial respiration and electron transport chain activity (39). However, using muscle cells, it has been shown that PGC1α increases the expression of one of the major antioxidant enzymes of mitochondria, SOD2 (40–42). PGC1α is therefore able to upgrade aerobic energy metabolism while preserving ROS homeostasis by promoting ROS formation on one hand and ROS scavenging systems on the other. If this is true for tissues with high aerobic energy demand, such as brain, heart, skeletal muscle,

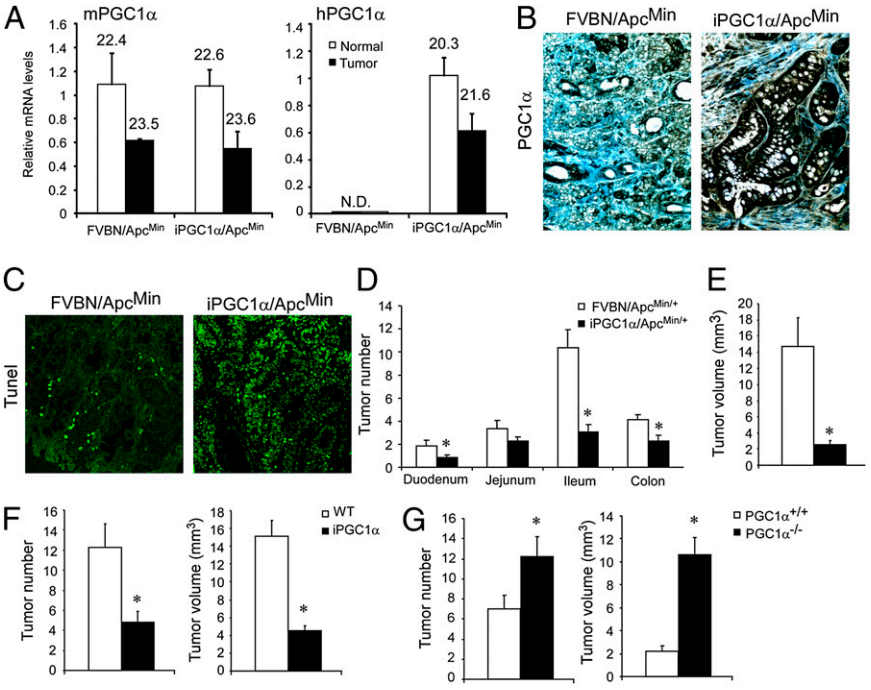

Fig. 5. Intestinal PGC1α prevents tumor formation. (*A*) Endogenous PGC1α (mPGC1α) and human transgene (hPGC1α) from intestinal tumors and normal mucosa of FVBN/Apc^{Min} and iPGC1α/Apc^{Min} mice were measured by real-time qPCR. Mean cycle threshold (Ct) values of intestinal tumors and normal mucosa are reported in number. The endogenous PGC1α as well as human transgene PGC1a (where detectable) are down-regulated in tumors from FVBN/Apc^{Min} and iPGC1α/Apc^{Min} mice. In tumors from iPGC1α/Apc^{Min} mice, human PGC1α is highly expressed as indicated by real-time average Ct values. (*B*) Paraffin-embedded adenoma specimens from FVBN/Apc^{Min} and iPGC1α/Apc^{Min} mice were immunoassayed with PGC1α antibody to determine expression of PGC1α protein (200× magnification). PGC1α is expressed at a higher level in iPGC1α/Apc^{Min} than in FVBN/Apc^{Min} tumors. (*C*) TUNEL assay on paraffin-embedded tumor samples from iPGC1α/Apc^{Min} and FVBN/Apc^{Min}. The overexpression of PGC1α in iPGC1α/Apc^{Min} tumors results in a significant increase in apoptosis compared with FVBN/Apc^{Min} tumors. (*D*) iPGC1α/ Apc$^{Min/+}$ and FVBN/ Apc$^{Min/+}$ 7-mo-old male mice (15 mice for each strain) were analyzed for the number of tumors in the four intestinal segments (duodenum, jejunum, ileum, and colon). (*E*) There were significant differences in tumor volumes between iPGC1α/ Apc$^{Min/+}$ and FVBN/Apc$^{Min/+}$ mice reported in the graphs. (*F*) The AOM/DSS model of colon carcinogenesis was used in both iPGC1α and WT 16-wk-old male mice. The protocol resulted in a higher tumor number, and higher volumes developed in WT than in iPGC1α mice. (*G*) The AOM/DSS model of colon carcinogenesis was used in PGC1α$^{+/+}$ and PGC1α$^{-/-}$ 6-wk-old male mice. The protocol resulted in a higher tumor number, and higher volumes developed in PGC1α$^{-/-}$ than in WT mice. Note that the different numbers and sizes of tumors between WT mice in *F* and *G* are due to their different pure strain control background in which transgenic mice have been generated (FVBN for iPGC1a and C57B6/J for PGC1a$^{-/-}$ mice).

and brown adipose tissues (6–9, 24, 25), in the intestine PGC1a is not able to induce the ROS scavenging systems.

The intestine represents the interface between the organism and its luminal environment, being constantly challenged by diet-derived oxidants as well as by endogenously generated ROS, which can induce serious damage to all biological molecules and cell structures (43). To preserve cellular integrity and tissue homeostasis, the intestine possesses several defense mechanisms, such as free radical scavenger enzymes CAT and SOD2. However, these antioxidant enzymes are unevenly distributed along the crypt-to-villus axis (Fig. S1*B*), being poorly expressed in the villus tip and leaving enterocytes unprotected against ROS damages and cell death (15). This uneven distribution likely renders the top of the villi and the surface epithelium weakly protected from ROS accumulation and therefore prone to regular cell turnover by apoptosis. In this study, we show that overexpression of PGC1α in tumors guarantees an increase in mitochondrial respiration and ROS production that is not linked with a sustained scavenger activity of SOD2, whose expression is actually decreased in tumors (Fig. S1*B*). Thus, PGC1α in vivo produces a significant delay in tumor growth rate. On the other hand, the absence of PGC1α produces an intestinal tumor-susceptible phenotype. We therefore present an intriguing scenario whereby PGC1α is a metabolic regulator of intestinal cell fate and protects against tumorigenesis by promoting mitochondrial-mediated apoptosis via ROS accumulation.

Methods

Cell Cultures. HT29 (HTB-38), C2C12, and 143B cells were obtained from ATCC (ATCC-LGC Promochem) and were maintained in DMEM supplemented with 10% FBS and 1% penicillin/streptomycin. The generation of HT29ρ0 cells is described in *SI Methods*.

Mice. Nude mice for the xenograft experiments were obtained from the Jackson Laboratory. The iPGC1α transgenic mice were generated by injection into the pronuclei of the fertilized eggs of the FVB/N mice. iPGC1α $Apc^{Min/+}$ mice were generated by crossing iPGC1α transgenic mice with C57BL/6-$Apc^{Min/+}$ mice (Jackson Laboratory). A straight knockout strategy, deleting exons 3–5, was used to target the *PGC1α* locus to generate mice carrying knockout alleles at this site. Details are reported in *SI Methods* and in Table S3 and Fig. S3. The ethics committee of the Consorzio Mario Negri Sud approved this experimental set-up.

ACKNOWLEDGMENTS. We are indebted to D. Gumucio, R. Mariani-Costantini, M. Plateroti, and R. Valanzano for their invaluable tools. We thank E. Bellafante, M. Cristofaro, A. D'Orazio, L. Evans, S. Modica, and M. Petruzzelli for their invaluable help during the study. We thank the Telethon Core Facility for Conditional Mutagenesis at the Istituto Scientifico San Raffaele (Milano) for generating the iPGC1α mice and the Telethon Electron Microscopy Core Facility at Consorzio Mario Negri Sud for the EM specimens. We thank Xiufeng Xu and coworkers at ATCG, AstraZeneca Mölndal for deriving the C57Bl/6JOlaHsd, AZX1, ES cell line. Support for this study was provided by Italian Association for Cancer Research Grant AIRC, IG 10416 (to A.M.), Italian Ministry of University Grant FIRB IDEAS RBID08C9N7, Italian Ministry of Health Young Researchers Grant GR-2008-1143546, the European Community's Seventh Framework Programme FP7/2007-2013 under Grant 202272 (LipidomicNet), Telethon Foundation Grant GPP08259, Cariplo Foundation Milan, Natural Pharma International, National Research Project PRIN 2006 no. 2006069034_004 of the Italian Ministry of the University (to G.V.), the Sächsische Ministerium für Wissenschaft und Kunst and the Bundesministerium für Bildung und Forschung (P.S.). S.M. is supported by a fellowship from CariSPAQ (L'Aquila, Italy). I.D. and G.L.S. are fellows of the Italian Association for Cancer Research.

1. Clevers H (2006) Wnt/beta-catenin signaling in development and disease. *Cell* 127: 469–480.
2. Rubinfeld B, et al. (1996) Binding of GSK3beta to the APC-beta-catenin complex and regulation of complex assembly. *Science* 272:1023–1026.
3. Morin PJ, Vogelstein B, Kinzler KW (1996) Apoptosis and APC in colorectal tumorigenesis. *Proc Natl Acad Sci USA* 93:7950–7954.
4. Kinzler KW, Vogelstein B (1996) Lessons from hereditary colorectal cancer. *Cell* 87:159–170.
5. Vogelstein B, Kinzler KW (2004) Cancer genes and the pathways they control. *Nat Med* 10:789–799.
6. Kelly DP, Scarpulla RC (2004) Transcriptional regulatory circuits controlling mitochondrial biogenesis and function. *Genes Dev* 18:357–368.
7. Wu Z, et al. (1999) Mechanisms controlling mitochondrial biogenesis and respiration through the thermogenic coactivator PGC-1. *Cell* 98:115–124.
8. Puigserver P, et al. (1998) A cold-inducible coactivator of nuclear receptors linked to adaptive thermogenesis. *Cell* 92:829–839.
9. Lin J, et al. (2002) Transcriptional co-activator PGC-1 alpha drives the formation of slow-twitch muscle fibres. *Nature* 418:797–801.
10. Puigserver P, Spiegelman BM (2003) Peroxisome proliferator-activated receptor-gamma coactivator 1 alpha (PGC-1 alpha): Transcriptional coactivator and metabolic regulator. *Endocr Rev* 24:78–90.
11. D'Aurelio M, et al. (2001) In vivo regulation of oxidative phosphorylation in cells harboring a stop-codon mutation in mitochondrial DNA-encoded cytochrome *c* oxidase subunit I. *J Biol Chem* 276:46925–46932.
12. Villani G, Greco M, Papa S, Attardi G (1998) Low reserve of cytochrome *c* oxidase capacity in vivo in the respiratory chain of a variety of human cell types. *J Biol Chem* 273:31829–31836.
13. Villani G, Attardi G (1997) In vivo control of respiration by cytochrome *c* oxidase in wild-type and mitochondrial DNA mutation-carrying human cells. *Proc Natl Acad Sci USA* 94:1166–1171.
14. Turan A, Mahmood A (2007) The profile of antioxidant systems and lipid peroxidation across the crypt-villus axis in rat intestine. *Dig Dis Sci* 52:1840–1844.
15. Turan A, Gill R, Dudeja PK, Mohan H, Mahmood A (2009) Effect of fat feeding on pro-oxidant and anti-oxidant enzyme systems in rat intestine: Possible role in the turnover of enterocytes. *Dig Dis Sci* 54:1229–1236.
16. Fodde R, Smits R, Clevers H (2001) APC, signal transduction and genetic instability in colorectal cancer. *Nat Rev Cancer* 1:55–67.
17. Bienz M, Clevers H (2000) Linking colorectal cancer to Wnt signaling. *Cell* 103:311–320.
18. Powell SM, et al. (1993) Molecular diagnosis of familial adenomatous polyposis. *N Engl J Med* 329:1982–1987.
19. Su LK, et al. (1992) Multiple intestinal neoplasia caused by a mutation in the murine homolog of the APC gene. *Science* 256:668–670.
20. Shakya A, et al. (2009) Oct1 loss of function induces a coordinate metabolic shift that opposes tumorigenicity. *Nat Cell Biol* 11:320–327.
21. Bonnet S, et al. (2007) A mitochondria-K+ channel axis is suppressed in cancer and its normalization promotes apoptosis and inhibits cancer growth. *Cancer Cell* 11:37–51.
22. Hájek P, Villani G, Attardi G (2001) Rate-limiting step preceding cytochrome *c* release in cells primed for Fas-mediated apoptosis revealed by analysis of cellular mosaicism of respiratory changes. *J Biol Chem* 276:606–615.
23. Reed JC (2003) Apoptosis-targeted therapies for cancer. *Cancer Cell* 3:17–22.
24. Lehman JJ, et al. (2000) Peroxisome proliferator-activated receptor gamma coactivator-1 promotes cardiac mitochondrial biogenesis. *J Clin Invest* 106:847–856.
25. St-Pierre J, et al. (2006) Suppression of reactive oxygen species and neurodegeneration by the PGC-1 transcriptional coactivators. *Cell* 127:397–408.
26. Christofk HR, et al. (2008) The M2 splice isoform of pyruvate kinase is important for cancer metabolism and tumour growth. *Nature* 452:230–233.
27. King MP, Attardi G (1989) Human cells lacking mtDNA: Repopulation with exogenous mitochondria by complementation. *Science* 246:500–503.
28. Rong Y, Doctrow SR, Tocco G, Baudry M (1999) EUK-134, a synthetic superoxide dismutase and catalase mimetic, prevents oxidative stress and attenuates kainate-induced neuropathology. *Proc Natl Acad Sci USA* 96:9897–9902.
29. Papanikolaou A, et al. (1998) Initial levels of azoxymethane-induced DNA methyl adducts are not predictive of tumor susceptibility in inbred mice. *Toxicol Appl Pharmacol* 150:196–203.
30. Popivanova BK, et al. (2008) Blocking TNF-alpha in mice reduces colorectal carcinogenesis associated with chronic colitis. *J Clin Invest* 118:560–570.
31. Drori S, et al. (2005) Hic-5 regulates an epithelial program mediated by PPARgamma. *Genes Dev* 19:362–375.
32. Arany Z, et al. (2008) HIF-independent regulation of VEGF and angiogenesis by the transcriptional coactivator PGC-1alpha. *Nature* 451:1008–1012.
33. Lefebvre AM, et al. (1998) Activation of the peroxisome proliferator-activated receptor gamma promotes the development of colon tumors in C57BL/6J-APCMin/+ mice. *Nat Med* 4:1053–1057.
34. Saez E, Olson P, Evans RM (2003) Genetic deficiency in Pparg does not alter development of experimental prostate cancer. *Nat Med* 9:1265–1266.
35. Sarraf P, et al. (1998) Differentiation and reversal of malignant changes in colon cancer through PPARgamma. *Nat Med* 4:1046–1052.
36. Modica S, Murzilli S, Salvatore L, Schmidt DR, Moschetta A (2008) Nuclear bile acid receptor FXR protects against intestinal tumorigenesis. *Cancer Res* 68:9589–9594.
37. Xiao JH, et al. (2003) Adenomatous polyposis coli (APC)-independent regulation of beta-catenin degradation via a retinoid X receptor-mediated pathway. *J Biol Chem* 278:29954–29962.
38. Modica S, et al. (2010) The intestinal nuclear receptor signature with epithelial localization patterns and expression modulation in tumors. *Gastroenterology* 138: 636–648, 648, e1–e12.
39. Murphy MP (2009) How mitochondria produce reactive oxygen species. *Biochem J* 417:1–13.
40. St-Pierre J, et al. (2003) Bioenergetic analysis of peroxisome proliferator-activated receptor gamma coactivators 1alpha and 1beta (PGC-1alpha and PGC-1beta) in muscle cells. *J Biol Chem* 278:26597–26603.
41. Valle I, Alvarez-Barrientos A, Arza E, Lamas S, Monsalve M (2005) PGC-1alpha regulates the mitochondrial antioxidant defense system in vascular endothelial cells. *Cardiovasc Res* 66:562–573.
42. Kukidome D, et al. (2006) Activation of AMP-activated protein kinase reduces hyperglycemia-induced mitochondrial reactive oxygen species production and promotes mitochondrial biogenesis in human umbilical vein endothelial cells. *Diabetes* 55:120–127.
43. Ames BN, Shigenaga MK, Hagen TM (1993) Oxidants, antioxidants, and the degenerative diseases of aging. *Proc Natl Acad Sci USA* 90:7915–7922.